



Contents lists available at ScienceDirect

Bioorganic & Medicinal Chemistry

journal homepage: www.elsevier.com/locate/bmc

Novel fluorine-18 labeled 5-(1-pyrrolidinylsulfonyl)-7-azaisatin derivatives as potential PET tracers for in vivo imaging of activated caspases in apoptosis

Christopher M. Waldmann^{a,*}, Sven Hermann^b, Andreas Faust^b, Burkhard Riemann^a, Otmar Schober^a, Michael Schäfers^{a,b,d}, Günter Haufe^{c,d}, Klaus Kopka^{a,†}

^a Department of Nuclear Medicine, University Hospital Münster, Albert-Schweitzer-Campus 1, Building A1, D-48149 Münster, Germany

^b European Institute for Molecular Imaging (EIMI), University of Münster, Waldeyerstraße 11, D-48149 Münster, Germany

^c Organic Chemistry Institute, University of Münster, Corrensstrasse 40, D-48149 Münster, Germany

^d Cells-in-Motion Cluster of Excellence (EXC 1003–CiM), University of Münster, Waldeyerstraße 15, D-48149 Münster, Germany

ARTICLE INFO

Article history:

Received 29 April 2015

Revised 1 July 2015

Accepted 9 July 2015

Available online xxx

Keywords:

Apoptosis

7-Azaisatin

Caspase inhibitor

Click-chemistry

¹⁸F-radiolabeling

Positron emission tomography (PET)

ABSTRACT

The programmed type I cell death, defined as apoptosis, is induced by complex regulated signaling pathways that trigger the intracellular activation of executioner caspases-3, -6 and -7. Once activated, these enzymes initiate cellular death through cleavage of proteins which are responsible for DNA repair, signaling and cell maintenance. Several radiofluorinated inhibitors of caspases-3 and -7, comprising a moderate lipophilic 5-(1-pyrrolidinylsulfonyl)isatin lead structure, are currently being investigated for imaging apoptosis in vivo by us and others. The purpose of this study was to increase the intrinsic hydrophilicity of the aforementioned lead structure to alter the pharmacokinetic behavior of the resulting caspase-3 and -7 targeted radiotracer. Therefore, fluorinated and non-fluorinated derivatives of 5-(1-pyrrolidinylsulfonyl)-7-azaisatin were synthesized and tested for their inhibitory properties against recombinant caspases-3 and -7. Fluorine-18 has been introduced by copper(I)-catalyzed azide-alkyne cycloaddition (CuAAC) of an alkyne precursor with 2-[¹⁸F]fluoroethylazide. Using dynamic micro-PET biodistribution studies in vivo the kinetic behavior of one promising PET-compatible 5-pyrrolidinylsulfonyl 7-azaisatin derivative has been compared to a previously described isatin based radiotracer.

© 2015 Elsevier Ltd. All rights reserved.

1. Introduction

Apoptosis is a form of programmed cell death in multicellular organisms.¹ In adult individuals cell homeostasis is achieved when the rate of mitotic cell division is balanced by cell death. However, apoptosis failure can contribute to profound pathologies such as tumor growth and autoimmune diseases whereas unwanted apoptosis occurs in many neurodegenerative disorders.² Apoptotic cell death is induced by complex regulated signaling pathways triggered by either activation of death receptors (extrinsic pathway) or mitochondria (intrinsic pathway).³ Both pathways activate the intracellular enzyme class of cysteinyl aspartate-specific proteases, in short caspases.⁴ Among these the executioner caspases-3, -6 and

-7, once activated, irrevocably initiate cellular death through cleavage of proteins which are responsible for DNA repair, signaling and cell maintenance. Therefore, these enzymes are suitable in vivo biomarkers of living apoptotic cells and tissues.

In 2000, Lee et al. described the discovery of 1-methyl-5-nitroisatin as a selective, non-peptidic inhibitor of recombinant caspase-3 showing a K_i value of 0.5 μM .⁵ In order to substitute the metabolically susceptible nitro group (*S*)-*N*-methyl-5-[1-(2-phenoxymethylpyrrolidinyl)sulfonyl]isatin was developed which retained high selectivity and inhibitory potency towards executioner caspases-3 and -7. X-ray crystallographic analysis of an enzyme-inhibitor complex revealed the binding mode of the inhibitor. It has been shown that the nucleophilic cysteine thiolate within the active site binds the carbonyl group in position 3 of the isatin covalently under formation of a tetrahedral thiohemiacetal. Selectivity towards caspases-3 and -7 is achieved by hydrophobic interactions between the pyrrolidine-moiety of the inhibitor and the S_2 binding pocket of the enzyme.

Based on these findings, structure-activity relationship studies were performed leading to an extensive compound library of

* Corresponding author at present address: Crump Institute for Molecular Imaging, Department of Molecular and Medical Pharmacology, David Geffen School of Medicine at UCLA, 570 Westwood Plaza, Los Angeles, CA 90095, United States. Tel.: +1 310 794 1731; fax: +1 310 206 8975.

E-mail address: cwaldmann@mednet.ucla.edu (C.M. Waldmann).

† Present address: Radiopharmaceutical Chemistry, German Cancer Research Center (dkfz), Im Neuenheimer Feld 280, D-69120 Heidelberg, Germany.

5-(1-pyrrolidinylsulfonyl)isatin derivatives.^{6–11} Mainly, side chains with different functionality were introduced either at position N1 of isatin or at position 2 of the pyrrolidine leading to highly selective inhibitors with K_i (or IC_{50}) values in the low nanomolar range.

To enable the use of 5-(1-pyrrolidinylsulfonyl)isatin derivatives for imaging of activated caspases in apoptosis, we and others introduced fluorine-18 to various sites of the inhibitor (Fig. 1).^{8,12–21} Fluorine-18 is a low energy positron emitter with a half life of ~110 min making it an ideal substituent to label molecular imaging probes for positron emission tomography (PET). PET-compatible derivatives of isatin derived caspase inhibitors show potential in monitoring apoptosis during cancer therapy.^{22,24}

A possible drawback of 5-(1-pyrrolidinylsulfonyl)isatin based apoptosis imaging agents concerns their pharmacokinetic behavior, which is mainly controlled by the moderate lipophilicity of the core skeletal structure. Biodistribution studies of fluorine-18 labeled derivatives in both rodents and humans often reveal a lower renal excretion compared to routinely used radiotracers such as 2-deoxy-2-[¹⁸F]fluoro-D-glucose ([¹⁸F]FDG).²³ The predominant clearance via the hepatobiliary route implicates a rather maintained circulation of the radiotracer over time which potentially supports undesired oxidative metabolism of any corresponding radiotracer.²⁵ Generally, prolonged biodistribution of radiotracers and its metabolites can increase unspecific binding to off-targets which in turn leads to an undesired low signal-to-noise ratio and higher background signal. Therefore, we intended to increase the inherent hydrophilicity of the isatin-based apoptosis imaging agents by envisioning second generation caspase-3 and -7 inhibitors based on a 7-azaisatin sulfonamide skeletal structure (Fig. 2).

Here, we report on the synthesis and in vitro evaluation of the caspase inhibition potencies of non-fluorinated and fluorinated derivatives of 5-(1-pyrrolidinylsulfonyl)-7-azaisatin. The fluorine-18 labeled substituent is introduced by copper(I)-catalyzed azide-alkyne cycloaddition (CuAAC).²⁶ This study will allow us to evaluate the impact of the hydrophilicity of the skeletal structure on the pharmacokinetic behavior of the corresponding radiotracer.

2. Results and discussion

2.1. Chemistry

According to Lee et al. 5-(1-pyrrolidinylsulfonyl)isatin based caspase inhibitors can be synthesized from isatin and (S)-proline

as starting materials.⁵ Therefore, isatin is sulfonated in position 5 using sulfur trioxide. The resulting sulfonate is converted into the corresponding sulfonyl chloride and subsequently coupled with an appropriate (S)-proline derivative to yield the inhibitor's core structure. Initially we attempted to adapt this methodology in order to synthesize an inhibitor of caspase-3 and -7 with a 7-azaisatin core. However, forming the sulfonate of 7-azaisatin in position 5 under various conditions was unsuccessful. This could be explained in part by the low electron density at the pyridine moiety of the molecule. In a next attempt to prepare the sulfonyl chloride of 7-azaisatin we adapted a known one-pot synthesis sequence starting with previously described 5-bromo-1-methyl-7-azaisatin (1) (Scheme 1).^{27,28}

The reaction sequence is composed of a bromine lithium exchange reaction by using 2.0 equiv *tert*-butyllithium (*t*-BuLi) at $-80\text{ }^\circ\text{C}$ in tetrahydrofuran (THF) (1), conversion of the resulting aryllithium with gaseous SO_2 to an arylsulfinate (2) and subsequent oxidation to the desired sulfonyl chloride with *N*-chlorosuccinimide (NCS) at room temperature in dichloromethane (DCM) (3). Analysis of the resulting complex mixture revealed that compound 2 was not formed under these conditions. In another attempt the reactive carbonyl function in position 3 of 7-azaisatin was protected as 1,3-dioxane beforehand, but still the desired product could not be isolated (reaction sequence not shown).

Therefore, we designed a new synthetic strategy starting with commercially available 5-bromo-7-azaindole (Scheme 2). This strategy aims at the formation of a 5-(1-pyrrolidinylsulfonyl)-7-azaindole skeletal structure and subsequent oxidation of the 7-azaindole moiety to 7-azaisatin. In order to prepare two N1-alkylated non-fluorinated 5-(1-pyrrolidinylsulfonyl)-7-azaisatin derivatives, position N1 was alkylated either with methyl iodide or *n*-propyl bromide, respectively. The two different alkyl substituents were chosen because of their favorable properties in regard to inhibition potency and cellular uptake.^{7,9} As shown in Scheme 2 we were able to prepare the 5-(1-pyrrolidinylsulfonyl)-7-azaindole derivatives 6 and 7 in a modified four step sequence. In previous protocols usually ≥ 2 equiv *t*-BuLi are used for a complete halogen-lithium exchange reaction.²⁹ The first equivalent is used for the exchange, and the second reacts with the produced *t*-BuBr to form isobutene, isobutane, and lithium bromide. We found that the use of just one equiv *t*-BuLi is sufficient and improves the reaction sequence in terms of reproducibility, atom efficiency and higher yields.³⁰ Furthermore, we were able to

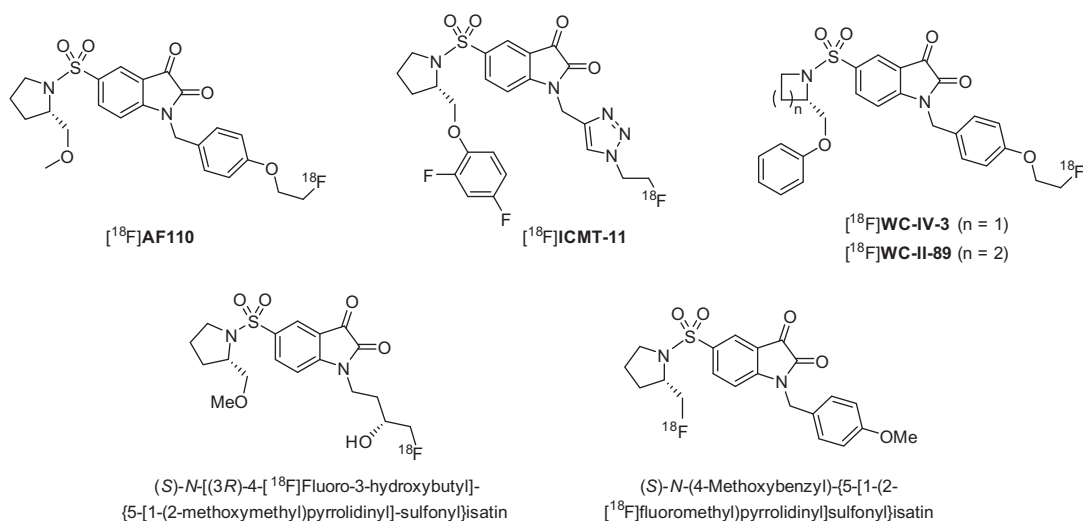


Figure 1. Selected 5-(1-pyrrolidinylsulfonyl)isatin based apoptosis imaging agents currently tested in preclinical studies.^{8,12,13,15,16,19,20} [¹⁸F]ICMT-11 was previously subjected to biodistribution and radiation dosimetry studies in humans.²³

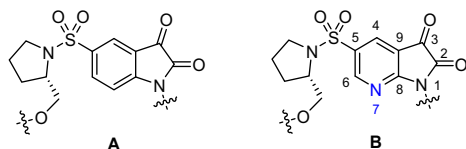
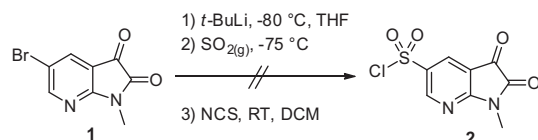


Figure 2. Core structures of hitherto existing inhibitors based on isatin (A) and envisioned 7-azaisatin based inhibitors of caspases-3 and -7 (B).



Scheme 1. Attempted one-pot synthesis of sulfonyl chloride **2**.

replace gaseous SO_2 with 1,4-diazabicyclo-[2.2.2]octane (DABCO)-bis(sulfur dioxide) (DABSO).³¹ This bench-stable colorless solid is easier to handle and allows a fully controlled dosing of SO_2 equivalents. After formation of the arylsulfinate by reacting DABSO with the organolithium compound the sulfonyl chloride was prepared with NCS. 2-Methoxymethyl-substituted pyrrolidine **5** was prepared according to literature procedure and used as an amine for the sulfonamide formation.⁷ Using this new protocol compounds **6** and **7** were synthesized in overall yields of 40% and 37%, respectively. Both compounds were easily oxidized by the use of CrO_3 to form desired 7-azaisatin derivatives **8** and **9** in fair yields.

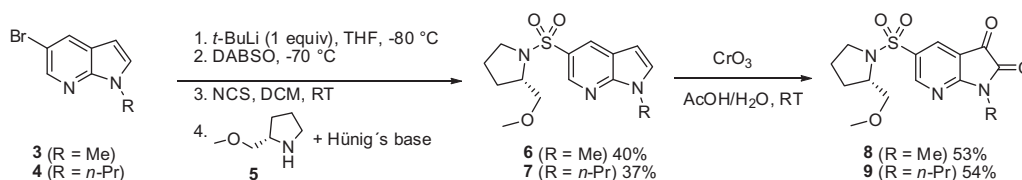
In order to enable the incorporation of 2-fluoroethylazide (**15**) or 2-[^{18}F]fluoroethylazide (^{18}F **15**) via CuAAC we conducted the synthesis of alkyne precursor **14** as depicted in Scheme 3. Starting with *N*-triisopropylsilyl (*N*-TIPS) protected 5-bromo-7-azaindole (**10**) we were able to prepare the 5-(1-pyrrolidinylsulfonyl)-7-azaindole skeletal structure **11** via an optimized four step one-pot synthesis in 64% yield. The silyl protecting group was smoothly removed with tetra-*n*-butylammonium fluoride (TBAF) under standard conditions. After propargylation of compound **12**

to yield alkyne **13**, CuAAC-precursor **14** was prepared by oxidation with CrO_3 as described before. The cycloaddition reaction of precursor **14** with 2-fluoroethylazide (**15**) to yield desired inhibitor **16** was accomplished under optimized 'click'-conditions but resulted in poor yields in several attempts.

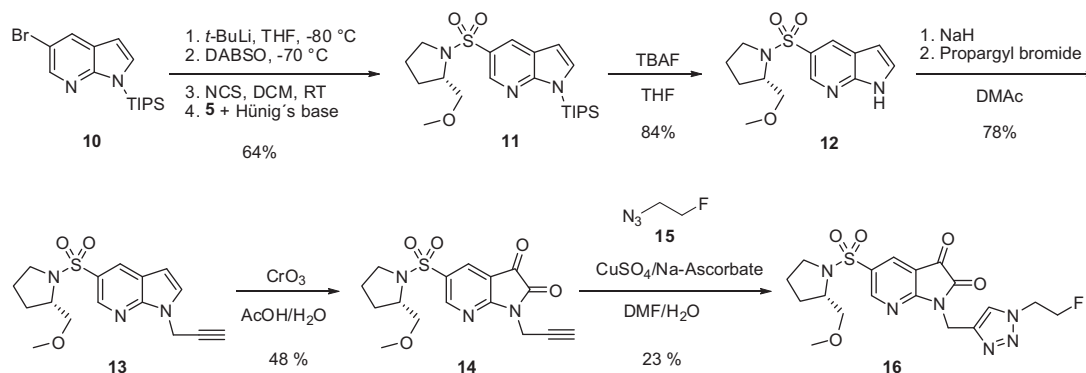
It has been shown that in case of 5-(1-pyrrolidinylsulfonyl)isatin based inhibitors of caspase-3 and -7 a 2'-fluoroethyl-1,2,3-triazole side chain can also be attached in position 2 of the pyrrolidine moiety without compromising on the inhibitory activity.⁸ Therefore, we planned to prepare a comparable 7-azaisatin derivative of type **20** (Scheme 4). In anticipation of higher inhibition potencies, we chose to attach the *n*-propyl substituent at N1 (see Table 1 in Section 2.2). The 7-azaindole skeletal structure **18** was prepared following the optimized one-pot synthesis conditions in 69% yield. Alkyne functionalized pyrrolidine **17** was prepared according to literature precedent.⁸ In this case the oxidation reaction with CrO_3 gave a higher yield of 67% of CuAAC-precursor **19** compared to corresponding precursor **14**. Additionally, despite similar reaction conditions, cycloaddition of alkyne **19** with 2-fluoroethylazide (**15**) gave considerably higher yields of inhibitor **20** (68% yield) compared to corresponding inhibitor **16** (23% yield).

2.2. Caspase inhibition potencies

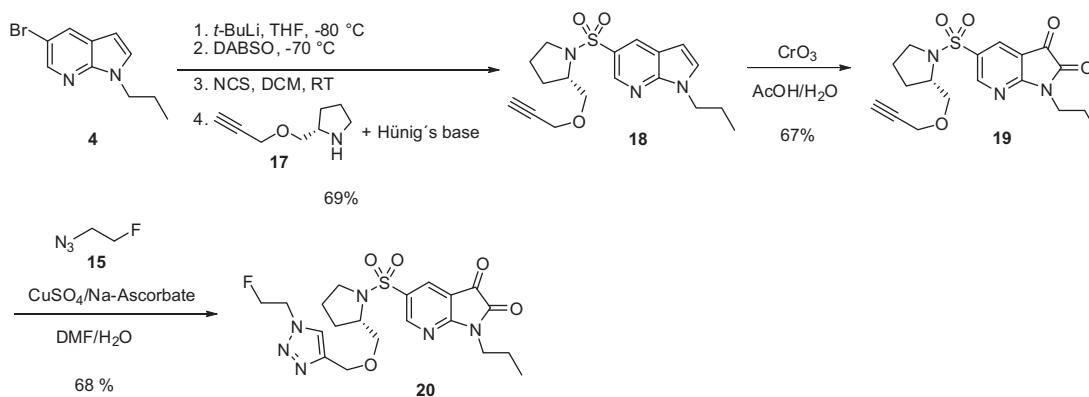
All synthesized non-fluorinated and fluorinated 7-azaisatin sulfonamides were tested *in vitro* as inhibitors of caspases-1, -3, -6 and -7 according to a published protocol.⁷ The resulting inhibition potencies are listed in Table 1. All tested inhibitors expressed inhibition potencies against effector caspases-3 and -7 in the nanomolar range ($\text{IC}_{50} = 17\text{--}501\text{ nM}$). A notable exception is the $\text{IC}_{50(\text{caspase } 3)} = 17,300\text{ nM}$ of compound **20**. Non-fluorinated inhibitor **8** exhibits a moderate inhibition potential of 429 nM (caspase 3) and 501 nM (caspase 7) which is comparable, yet lower, to the known corresponding isatin based inhibitor in which the nitrogen in position 7 is replaced by a CH-group ($\text{IC}_{50(\text{caspase } 3)} = 2\text{ nM}$ and $\text{IC}_{50(\text{caspase } 7)} = 304\text{ nM}$).⁷ The differences in the inhibition potencies of 7-azaisatin inhibitor **8** and its previously described isatin counterpart⁷ could in part be explained by their differing hydrophilicity.



Scheme 2. Synthesis of fluorine-free 5-(1-pyrrolidinylsulfonyl)-7-azaisatin derivatives **8** and **9**.



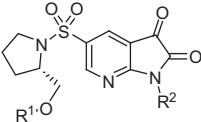
Scheme 3. Synthesis of CuAAC-precursor **14** and fluorinated 5-(1-pyrrolidinylsulfonyl)-7-azaisatin derivative **16**.



Scheme 4. Synthesis of CuAAC-precursor **19** and fluorinated 5-(1-pyrrolidinylsulfonyl)-7-azaisatin derivative **20**.

Table 1

Caspase inhibition potencies of synthesized 7-azaisatin sulfonamides towards caspases-1, -3, -6 and -7 expressed as IC_{50} values (nM)



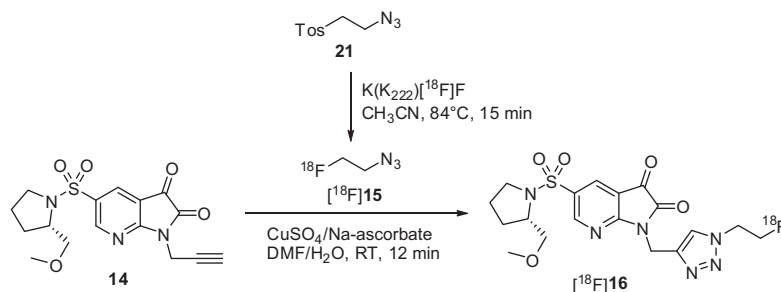
Inhibitor	R ¹	R ²	Caspase inhibition potencies IC_{50} (nM)			
			Caspase-1	Caspase-3	Caspase-6	Caspase-7
8	Me	Me	>50,000	429 ± 374	>50,000	501 ± 25
9	Me	<i>n</i> -Pr	>50,000	83 ± 10	>50,000	75 ± 12
16	Me	[1-(2-Fluoroethyl)-1,2,3-triazol-4-yl]methyl	>50,000	21 ± 2	>50,000	97 ± 13
20	[1-(2-Fluoroethyl)-1,2,3-triazol-4-yl]methyl	<i>n</i> -Pr	>50,000	17,300 ± 3110	>50,000	17 ± 2

The hydrophilicity of a compound can be indicated by its calculated octanol/water partition coefficient ($clogD$) which is 0.28 for the isatin- and -1.39 for the 7-azaisatin derivative, respectively, showing the considerable impact of the 7-azaisatin moiety on the water solubility. Moreover, a modified receptor–ligand interaction of phenyl and pyridyl moieties due to increased electron density in 7-position might contribute to the decreased potency. This argument is encouraged by our previous finding that the potency of *N*-alkyl isatins halogenated at the 7-position drops as compared to the corresponding unsubstituted compounds.⁹ Thus, increased electron density in the 7-position seems to result in modified receptor–ligand interactions. The *n*-propyl substituent of compound **9** increases the inhibition potencies against caspases-3 and -7. The IC_{50} values of the already known analog isatin compound are in the same order of magnitude ($IC_{50(\text{caspase } 3)} = 5$ nM and $IC_{50(\text{caspase } 7)} = 58$ nM). This is also true for a series of 7-halo isatin derivatives.⁹ Fluorinated 7-azaisatin compound **16** is a potent inhibitor of caspases-3 and -7 which is underlined by the corresponding IC_{50} values 21 nM and 97 nM, respectively. Once

more, the inhibition potencies of the corresponding analog isatin-**16** (see [Supporting information](#)) are higher ($IC_{50(\text{caspase } 3)} = 2$ nM and $IC_{50(\text{caspase } 7)} = 2$ nM). Notably, compound **16** comprises the lowest $clogD$ value of -1.88 of all compounds tested indicating its comparably high water solubility. The highest caspase-7 inhibition potency is observed for compound **20**, however, there is an unexpected drop of the IC_{50} value against caspase-3 to 17,300 nM. A comparable isatin sulfonamide analog which corresponds to the 7-azaisatin derivative **20** could not be found in literature.

2.3. Radiosynthesis

Radiosynthesis is accomplished using the same CuAAC methodology as described for the preparation of the nonradioactive azaisatin derivatives **16** and **20** (Section 2.1). Prosthetic group 2-[¹⁸F]fluoroethylazide ([¹⁸F]**15**) was synthesized by automated nucleophilic radiofluorination of 2-azidoethyl-4-methylbenzenesulfonate (**21**) and could be isolated by distillation in 60 ± 6% decay



Scheme 5. Radiosynthesis of [¹⁸F]**16** by CuAAC of a corresponding alkyne precursor **14** with 2-[¹⁸F]fluoroethylazide [¹⁸F]**15**.

corrected radiochemical yields (d.c. rcy, $n = 6$) (Scheme 5).³² The cycloaddition to yield desired compound [^{18}F]**16** was conducted outside the automated radiosynthesizer by reacting alkyne precursor **14** with [^{18}F]**15** in the presence of copper sulfate and sodium ascorbate. After purification by semipreparative HPLC and subsequent formulation, [^{18}F]**16** was obtained in an overall rcy of $11 \pm 5\%$ (d.c., $n = 5$) in 94 ± 12 min from the end of radionuclide production. Radiochemical purity was $94 \pm 5\%$ and the determined specific activities were in the range of $0.2\text{--}9.5$ GBq/ μmol . In order to determine the octanol/water partition coefficient at physiological pH ($\log D_{7.4}$) [^{18}F]**16** was formulated in phosphate buffered saline (PBS).³³ The measurement revealed a $\log D_{7.4}$ value of -1.32 which is in agreement with the calculated value of -1.88 .

Compound [^{18}F]**20** was prepared by using the same synthetic protocol as for [^{18}F]**16** starting with alkyne precursor **19**. After

formulation [^{18}F]**20** was prepared in $21 \pm 0\%$ rcy (d.c., $n = 2$) in 91 ± 9 min from the end of radionuclide production. Radiochemical purity was $>99\%$ and the determined specific activities were in the range of $0.2\text{--}0.3$ GBq/ μmol . The $\log D_{7.4}$ value was determined to be -0.01 ($\text{clog}D = -0.49$).

2.4. In vivo biodistribution studies

For biodistribution studies in wild-type mice (C57Bl/6, 11–12 weeks, 19–21 g body weight), we have chosen the most promising 7-azaisatin derived caspase-3 and -7 inhibitor [^{18}F]**16**. Dynamic PET scans in combination with computed tomography (CT) were used to obtain a series of images reflecting the radiotracer distribution at different time frames after injection (Fig. 3). Quantitative analysis (Fig. 4) revealed a fast washout of the radioactivity from

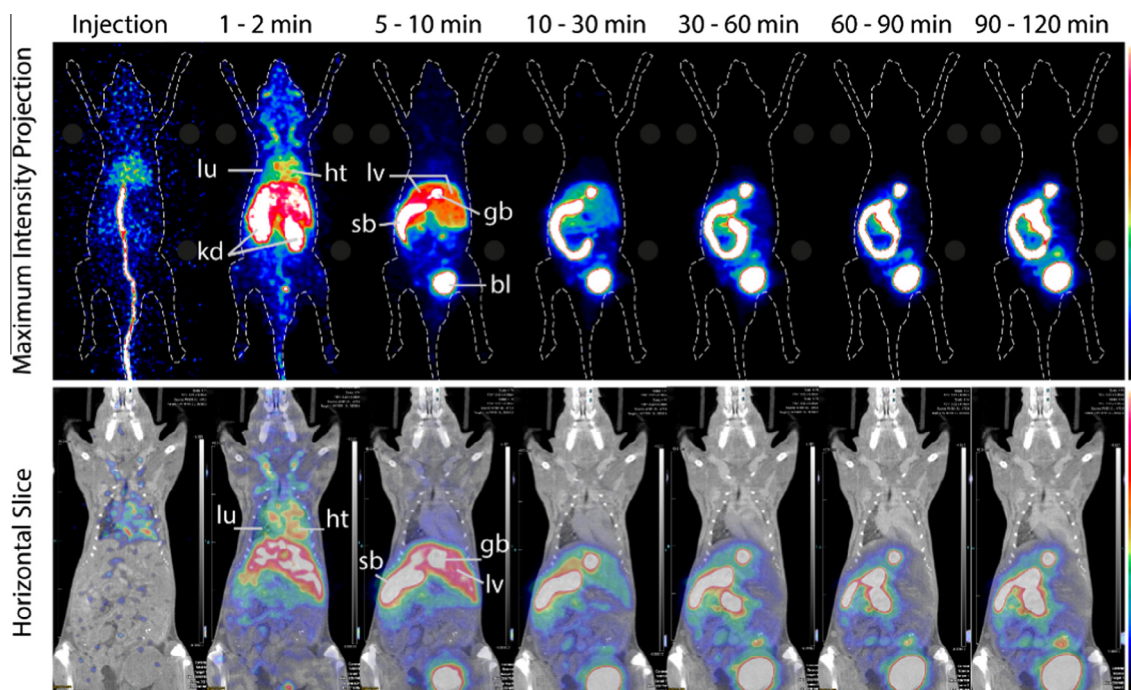


Figure 3. Biodistribution of radioactivity in an adult C57/BL6 mouse after intravenous injection of [^{18}F]**16** visualized by small-animal PET. Maximum intensity projections (MIP, first row) of selected time frames depict rapid hepatobiliary and renal excretion of [^{18}F]**16**. Whole-body horizontal slices from fused PET/CT imaging (one selected slice, second row) allow for better anatomical correlation and localization of radioactivity. Labeled structures are as follows: lung (lu), heart (ht), liver (lv), gallbladder (gb), small bowel (sb), kidneys (kd), and urinary bladder (bl).

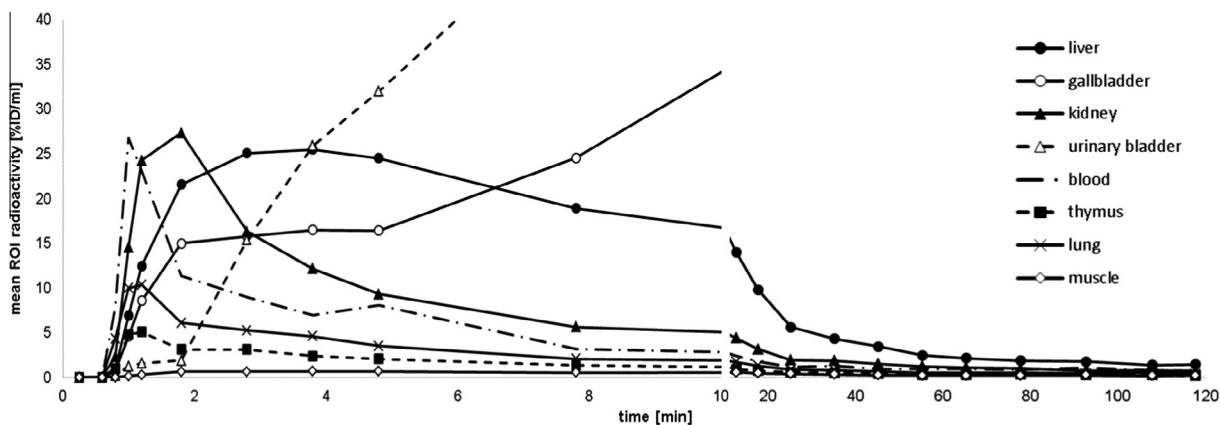


Figure 4. Representative time-activity concentration curves illustrating the rapid clearance of [^{18}F]**16** from the blood due to hepatobiliary and renal tracer elimination. Control region of interest (ROI) in reference tissues (thymus, lung, muscle) show low levels of radioactivity according to their blood fraction but no tracer accumulation.

Table 2
Elimination characteristics of [¹⁸F]AF110 and [¹⁸F]16 within 90 min

Tracer	cLogD	Elimination		
		Total (% injected activity)	Hepatobiliary (%)	Renal (%)
[¹⁸ F]AF110 ^a	2.20	63 ± 3	96 ± 1	4 ± 1
[¹⁸ F]16 ^b	−1.88	82 ± 2	68 ± 1	32 ± 1

^a (n = 3), biodistribution data of [¹⁸F]AF110 in [Supporting information](#).

^b (n = 2).

the blood, resulting in a blood activity comparable to background levels within 10 min. The tracer is rapidly eliminated via liver and kidneys and accumulates in gallbladder and bladder, respectively. In order to examine the influence of the more hydrophilic 7-azaisatin skeletal structure on the pharmacokinetic behavior in vivo, we compared the distribution data obtained from previously described isatinsulfonamide [¹⁸F]AF110 (IC₅₀ (caspase 3) = 36 nM and IC₅₀ (caspase 7) = 93 nM)¹² and [¹⁸F]16 (Table 2).

These results demonstrate an explicit difference in the elimination characteristics of both radiotracers. Within the observed time span of 90 min, 63 ± 3% injected activity of [¹⁸F]AF110 were eliminated via the organs of excretion (see [Supporting information](#)). In comparison, clearance of 7-azaisatin derivative [¹⁸F]16 was more efficient with a total of 82 ± 2% eliminated activity, implying a shorter retention time of the tracer in the organism. Notably, the fraction of tracer excreted via the kidneys was more pronounced using [¹⁸F]16 (32 ± 1%) as compared to [¹⁸F]AF110 (4 ± 1%). The reasons for the observed differences can be manifold. The overall higher hydrophilicity of 7-azaisatin derivative [¹⁸F]16 might contribute to the increased renal elimination and faster washout. Also, it is likely that [¹⁸F]16, as it is the case for [¹⁸F]AF110, forms metabolites in vivo that have a strong effect on the observed activity distribution.²⁵

3. Conclusion

PET-compatible fluorine-18 labeled 5-(1-pyrrolidinylsulfonyl)isatin derivatives are considered as putative in vivo apoptosis imaging agents. In order to influence the pharmacokinetic behavior of this class of radiotracers, we introduced a second generation lead structure in which the isatin moiety is replaced by 7-azaisatin. The syntheses of non-fluorinated and fluorinated 5-(1-pyrrolidinylsulfonyl)-7-azaisatin derivatives are described. All synthesized substances were tested for their inhibitory activity against caspases-1, -3, -6 and -7. While not being as potent as their isatin counterparts, the 7-azaisatin derivatives revealed satisfactory IC₅₀ values against caspases-3 and -7 in the nanomolar scale. PET-compatible fluorine-18 labeled tracers were prepared in a semi-automated radiosynthesis based on the CuAAC strategy. Compared to a previously described isatin PET tracer, the novel 7-azaisatin PET tracer exhibits an increased renal excretion in rodents and is cleared more efficiently from all organs investigated. These results demonstrate that 5-(1-pyrrolidinylsulfonyl)-7-azaisatin derivatives have the potential to be further developed as PET tracers for imaging of activated caspases in apoptosis. In future work, we plan to investigate whether or not the caspase-3 and -7 inhibitors described in this study can accumulate over time in living apoptotic cells with upregulated caspase-3 activity. Furthermore, compounds [¹⁸F]16 and [¹⁸F]AF110 will be tested in experimental models of increased apoptosis. We anticipate that the more efficient clearance of [¹⁸F]16 will result in a higher signal-to-noise ratio as well as a decreased background signal when compared to [¹⁸F]AF110.

Acknowledgments

These investigations were supported by the Deutsche Forschungsgemeinschaft (DFG), Collaborative Research Centre (SFB) 656 ‘Molecular Cardiovascular Imaging’, Projects A3, B1 and Z2.

Supplementary data

Supplementary data (synthetic procedures, spectroscopic data, in vitro caspase inhibition experiments, in vivo data, and copies of NMR spectra) associated with this article can be found, in the online version, at <http://dx.doi.org/10.1016/j.bmc.2015.07.014>.

References and notes

- Kerr, J. F.; Wyllie, A. H.; Currie, A. R. *Br. J. Cancer* **1972**, *26*, 239.
- Brunner, T.; Mueller, C. *Essays Biochem.* **2003**, *39*, 119.
- Hengartner, M. O. *Nature* **2000**, *407*, 770.
- Li, J.; Yuan, J. *Oncogene* **2008**, *27*, 6194.
- Lee, D.; Long, S. A.; Adams, J. L.; Chan, G.; Vaidya, K. S.; Francis, T. A.; Kikly, K.; Winkler, J. D.; Sung, C. M.; Debouck, C.; Richardson, S.; Levy, M. A.; DeWolf, W. E., Jr.; Keller, P. M.; Tomaszek, T.; Head, M. S.; Ryan, M. D.; Haltiwanger, R. C.; Liang, P. H.; Janson, C. A.; McDevitt, P. J.; Johanson, K.; Concha, N. O.; Chan, W.; Abdel-Meguid, S. S.; Badger, A. M.; Lark, M. W.; Nadeau, D. P.; Suva, L. J.; Gowen, M.; Nuttall, M. E. *J. Biol. Chem.* **2000**, *275*, 16007.
- Chu, W.; Zhang, J.; Zeng, C.; Rothfuss, J.; Tu, Z.; Chu, Y.; Reichert, D. E.; Welch, M. J.; Mach, R. H. *J. Med. Chem.* **2005**, *48*, 7637.
- Kopka, K.; Faust, A.; Keul, P.; Wagner, S.; Breyholz, H. J.; Höltke, C.; Schober, O.; Schäfers, M.; Levkau, B. *J. Med. Chem.* **2006**, *49*, 6704.
- Smith, G.; Glaser, M.; Perumal, M.; Nguyen, Q. D.; Shan, B.; Arstad, E.; Aboagye, E. O. *J. Med. Chem.* **2008**, *51*, 8057.
- Podichetty, A. K.; Faust, A.; Kopka, K.; Wagner, S.; Schober, O.; Schäfers, M.; Haufe, G. *Bioorg. Med. Chem.* **2009**, *17*, 2680.
- Podichetty, A. K.; Wagner, S.; Faust, A.; Schäfers, M.; Schober, O.; Kopka, K.; Haufe, G. *Future Med. Chem.* **2009**, *1*, 969.
- Limpachayaporn, P.; Schäfers, M.; Schober, O.; Kopka, K.; Haufe, G. *Bioorg. Med. Chem.* **2013**, *21*, 2025.
- Faust, A.; Wagner, S.; Law, M. P.; Hermann, S.; Schnöckel, U.; Keul, P.; Schober, O.; Schäfers, M.; Levkau, B.; Kopka, K. *Q. J. Nucl. Med. Mol. Imaging* **2007**, *51*, 67.
- Zhou, D.; Chu, W.; Chen, D. L.; Wang, Q.; Reichert, D. E.; Rothfuss, J.; D'Avignon, A.; Welch, M. J.; Mach, R. H. *Org. Biomol. Chem.* **2009**, *7*, 1337.
- Podichetty, A. K.; Wagner, S.; Schröer, S.; Faust, A.; Schäfers, M.; Schober, O.; Kopka, K.; Haufe, G. *J. Med. Chem.* **2009**, *52*, 3484.
- Chen, D. L.; Zhou, D.; Chu, W.; Herrbrich, P. E.; Jones, L. A.; Rothfuss, J. M.; Engle, J. T.; Geraci, M.; Welch, M. J.; Mach, R. H. *Nucl. Med. Biol.* **2009**, *36*, 651.
- Chen, D. L.; Zhou, D.; Chu, W.; Herrbrich, P. E.; Engle, J. T.; Griffin, E.; Jones, L. A.; Rothfuss, J. M.; Geraci, M.; Hotchkiss, R. S.; Mach, R. H. *Nucl. Med. Biol.* **2012**, *39*, 137.
- Nguyen, Q. D.; Challapalli, A.; Smith, G.; Fortt, R.; Aboagye, E. O. *Eur. J. Cancer* **2012**, *48*, 432.
- Limpachayaporn, P.; Riemann, B.; Kopka, K.; Schober, O.; Schäfers, M.; Haufe, G. *Eur. J. Med. Chem.* **2013**, *64*, 562.
- Limpachayaporn, P.; Wagner, S.; Kopka, K.; Hermann, S.; Schäfers, M.; Haufe, G. *J. Med. Chem.* **2013**, *56*, 4509.
- Krause-Heuer, A. M.; Howell, N. R.; Metesc, L.; Dhand, G.; Young, E. L.; Burgess, L.; Jiang, C. D.; Lengkeek, N. A.; Fookes, C. J. R.; Pham, T. Q.; Sobrio, F.; Greguric, I.; Fraser, B. H. *Med. Chem. Commun.* **2013**, *4*, 347.
- Limpachayaporn, P.; Wagner, S.; Kopka, K.; Schober, O.; Schäfers, M.; Haufe, G. *J. Med. Chem.* **2014**, *57*, 9383.
- Nguyen, Q. D.; Smith, G.; Glaser, M.; Perumal, M.; Arstad, E.; Aboagye, E. O. *Proc. Natl. Acad. Sci. U.S.A.* **2009**, *106*, 16375.
- Challapalli, A.; Kenny, L. M.; Hallett, W. A.; Kozlowski, K.; Tomasi, G.; Gudi, M.; Al-Nahhas, A.; Coombes, R. C.; Aboagye, E. O. *J. Nucl. Med.* **2013**, *54*, 1551.
- Witney, T. H.; Fortt, R. R.; Aboagye, E. O. *PLoS One* **2014**, *9*, e91694.
- Baumann, A.; Faust, A.; Law, M. P.; Kuhlmann, M. T.; Kopka, K.; Schäfers, M.; Karst, U. *Anal. Chem.* **2011**, *83*, 5415.
- Glaser, M.; Arstad, E. *Bioconjugate Chem.* **2007**, *18*, 989.
- Mader, M. M.; Shih, C.; Considine, E.; De Dios, A.; Grossman, C. S.; Hipskind, P. A.; Lin, F. S.; Lobb, K. L.; Lopez, J.; Lopez, J. E.; Cabrejas, L. M. M.; Richett, M. E.; White, W. T.; Cheung, Y. Y.; Huang, Z. P.; Reilly, J. E.; Dinn, S. R. *Bioorg. Med. Chem. Lett.* **2005**, *15*, 617.
- Tatsugi, J.; Tong, Z. W.; Tsuchiya, Y.; Ito, T. *ARKIVOC* **2009**, 132.
- Seebach, D.; Neumann, H. *Chem. Ber.* **1974**, *107*, 847.
- Waldmann, C.; Schober, O.; Haufe, G.; Kopka, K. *Org. Lett.* **2013**, *15*, 2954.
- Woolven, H.; González-Rodríguez, C.; Marco, I.; Thompson, A. L.; Willis, M. C. *Org. Lett.* **2011**, *13*, 4876.
- Schrigten, D.; Breyholz, H. J.; Wagner, S.; Hermann, S.; Schober, O.; Schäfers, M.; Haufe, G.; Kopka, K. *J. Med. Chem.* **2012**, *55*, 223.
- Prante, O.; Hocke, C.; Löber, S.; Hübner, H.; Gmeiner, P.; Kuwert, T. *Nuklearmedizin* **2006**, *45*, 41.